Reduced Graphene Oxide Films as Solid Transducer in Potentiometric All-Solid-State Ion-Selective Electrodes

Rafael Hernández,[a] Jordi Riu,[a] Johan Bobacka,[b] Cristina Vallés,[c] Pablo Jiménez,[c] Ana M. Benito,[c] Wolfgang K. Maser,[c] and F. Xavier Rius[a]*

[a] Department of Analytical and Organic Chemistry, Universitat Rovira i Virgili, Tarragona, Spain

[b] Laboratory of Analytical Chemistry, Process Chemistry Centre, Åbo Akademi University, Turku-Åbo, Finland

[c] Department of Chemical Processes and Nanotechnology, Instituto de Carboquímica ICB-CSIC, Zaragoza, Spain

RECEIVED DATE

*Corresponding author: e-mail: jordi.riu@urv.cat

ABSTRACT: The development of ion-selective electrodes (ISEs) using solid-state transducer materials is of great interest for advanced potentiometric detection systems. At present, conducting polymers are the most used solid-state transducing materials. However, their reliability is strongly related to their chemical stability and the formation of internal water films. Here we report on the use of reduced graphene oxide (RGO)

films of different thicknesses as transducer material in potentiometric all-solid-state ISE. First, the transduction mechanism is fully analysed revealing that RGO films act as asymmetric capacitors where its electron density is in contact with ions of the electrolyte solution creating a capacitance due to the constant phase elements present in the system. Second, as a proof of concept, RGO films are used in a calcium ISE showing highly reproducible sensing responses and outstanding increased signal-to-noise ratios with drifts of only 10 µV/h. These performance parameters are among the best compared to other ISE transducer materials so far. Combined with its ease of fabrication and processing into reproducible films of controlled thickness, ease for further tailoring chemical composition and tailoring electrical properties, RGO offers great promise as reliable high-performance transducer material for solid-state ISE sensors.

INTRODUCTION

Graphene is a one-atom thick two-dimensional sheet of sp^2 hybridized carbon that has excellent and unique thermal,[1] optical,[2] mechanical,[3] electronic[4] and electrochemical[5-9] properties. It is a promising candidate for next-generation devices such as transistors,[4] supercapacitors,[5] solar cells,[10] liquid crystal displays[11] and bio fuel cells.[12] Versatile and large-scale assembly is offered by solution based strategies.[13,14] While graphene itself is insoluble, chemically modified graphene (CMG) emerges as a valuable alternative.[14] To this end, graphene oxide (GO) is one of the most promising CMGs.[15] It can be described as a graphene sheet containing oxygen functional groups such as epoxides, alcohols, and carboxylic acids at its basal plane and edges.[16] It easily can be made from graphite oxide, which readily exfoliates as single GO sheets in water forming stable aqueous dispersions.[15,17] These can be used to fabricate macroscopic assemblies, such as continuous GO films. While GO itself is insulating due to the numerous oxygen

functional groups disrupting the sp^2 character of the carbon network, chemical reduction largely can restore the conductivity by several orders of magnitude by removal of oxygen and recovery of aromatic double-bonded carbons.[15] The applied reduction step controls the conductivity and number of remaining oxygen groups in the resulting reduced graphene oxide (RGO). Being conducting, easily processable into thin films and not possessing any metallic impurities (as is the case for carbon nanotubes) renders RGO of great interest for the fabrication of transducers in different kind of sensors.[18-21]

Electrochemical detection techniques have a series of advantages such as rapid response, ease of use, low-cost and small sized commercial detectors. Amperometric sensing devices based on graphene have already been reported for the detection of NO_2, NH_3, 2,4-dinitrotoluene,[22,23] cadmium[24] and dopamine[25]. Among the electrochemical techniques, potentiometry is one of the simplest, cost-efficient and most available detection systems worldwide. Within potentiometric techniques, ion-selective electrodes (ISEs) are the most commonly used sensing devices.

Current ISEs have evolved from the first ISEs based on internal solutions to all-solid-state ISEs. Solid state ISEs eliminate the internal solution incorporating a solid transducer between the ion-selective membrane and the conducting wire, paving the way for the development of a fully-miniaturized device. One of the most used solid transducers in ISEs are conductive polymers.[26] Although these transducing materials showed benefits compared to classical electrodes using internal solution, there were also some drawbacks such as the formation of internal water films,[27] sensitivity to light,[28] sensitivity to oxygen, CO_2 and pH.[29] These problems have encouraged the use of other transducing materials such as three-dimensionally ordered macroporous (3DOM) carbon,[30] single-walled carbon nanotubes (SWCNTs)[31] or multi-walled carbon nanotubes (MWCNTs)[32] which offer a high potential stability in time, insensitivity to

oxygen and light, and the absence of a layer of water because of the hydrophobicity of these materials. The availability of chemically modified graphene (CMG) with its processing advantages and the absence of additional metallic impurities affecting the device response puts this material under scrutiny for improving the performance of ISEs. Very recently Ping et al.[33] reported for the first time the use of reduced graphene oxide (RGO) as an effective ion-to-electron transducer in potassium ISEs. They used a similar method of preparation of RGO as the one we use in this paper (they obtain RGO prior to the deposition over a glassy carbon electrode while in our case the reduction of GO to RGO is performed when the GO is already deposited on the glassy carbon electrode; see the Experimental Section), but using much lower volumes and concentrations of RGO which may give rise to problems in homogeneously covering the surface of the glassy carbon electrode. Furthermore the authors do not give information about the thickness of the RGO layer. Li et al.[34] also presented a potassium ISE using GO as solid transducer. But in this case it is not clear whether the authors reduced GO to form RGO so the transducer they use may be different from the one we use in this paper. Jaworska et al.[35,36] used carboxy-functionalized graphene in the construction of ISEs. They conclude that analytical parameters of carboxy-functionalized graphene ISEs are comparable to ISEs constructed with other solid-state transducers. But again their carboxy-functionalized graphene is different to the RGO we use in this paper since apparently the exfoliation procedure is not so thorough as the one we use (ultrasonication and centrifugation are not listed in their experimental procedure), and they do not seem to apply the reduction process with hydrazine vapours that we perform to obtain RGO (see our detailed procedure in 'Electrode Preparation' in the Experimental Section). All these ISEs made using different types of CMGs (which may have different chemical composition and may also have different mechanisms of

transduction) show the need of a deep and thorough characterization of these materials in order to be able to clearly and unambiguously compare the different sensors based on different CMGs.

In this paper we present the use of RGO films of well-defined thicknesses as transducers in potentiometric solid-state calcium ISEs. First we thoroughly studied for the first time the transduction mechanism of RGO films of three different thicknesses by using cyclic voltammetry (CV), electrochemical impedance spectroscopy (EIS) and equivalent circuit analysis using five different electrolytes. Second, as a proof of concept, we fully characterised the sensing performance (time response, linear range, detection limit, stability, selectivity, water-layer test) of the calcium ISE for 6 different electrodes and over a time window of more than 1 month. We show that RGO films with a homogeneous electrode coverage act as asymmetric capacitors offering Nernstian response, high sensor sensitivity and stability. Ease in the fabrication of RGO films with controlled thickness thus facilitates the fabrication of reliable and high performance solid-state ISE sensors.

EXPERIMENTAL SECTION

Reagents and samples. Fluka provided Ca^{2+}-selective ionophore N,N,N'-N'-tetraciclohexyl-3-oxapentanediamide (ETH129), reagent grade benzene, tetrahydrofuran (THF), potassium tetrakis[3,5-bis-(trifluoromethyl)phenyl]borate (KTFPB) and azobisisobutyronitrile initiator (AIBN). Methyl metacrylate (MMA), n-butyl acrylate (nBA), dichloromethane (DCM), ethanol, acetone, petroleum ether high boiling point (high boiling point: 80–100 ºC), dimethylformamide (DMF), sodium nitrate ($NaNO_3$), sulphuric acid (H_2SO_4), potassium permanganate ($KMnO_4$), hydrazine monohydrate and graphite powder were purchased from Sigma-Aldrich. Aqueous solutions were prepared

with freshly deionized water (18.2 MΩ·cm specific resistance) obtained with a Milli-Q PLUS reagent-grade water system (Millipore). Abrasive papers and alumina were obtained from Buehler. Glassy carbon rods 3 mm diameter were purchased from HTW GmbH.

Apparatus and procedures. Environmental scanning electron microscope (ESEM) images were taken with a Quanta 600 (FEI Company, Inc.) microscope. High-resolution transmission electronic (HR-TEM) images were taken on a FEI Tecnai G2 20 microscope. Confocal microscopy LEICA Dual Core 3D measuring Microscope 3D equipment was used to control the thickness of reduced graphene oxide (RGO) depositions. Scanning electronic microscopy (SEM) images were obtained in a Hitachi S-3400N microscope, and the AFM used was a Multimode 8 microscope with control electronics Nanoscope V (Bruker). X-Ray photoelectron spectroscopy (XPS) was carried out on an ESCAPlus Omicron spectrometer using a monochromatized Mg X-ray source (1253.6 eV). XPS data were analyzed using the CasaXPS software. A high input impedance electrometer 6514 from Keithley and an Autolab PGSTAT 128N from Eco Chemie, were used for potentiometric and impedance measurements, respectively. All the experiments were done at room temperature (22.0±0.1ºC) in a bath from Polyscience (ref.9106) with the same double-junction Ag/AgCl/ 3 M KCl reference electrode (type 6.0729.100, Methrom AG) containing a 1 M LiAcO electrolyte bridge. The same cell was used for the measurements in all the experiments in order to ensure that each experiment was carried out under the same conditions. The auxiliary electrode used in voltammetry, impedance and chronopotentiometry measurements was a glassy carbon rod and the reference electrode was a single-junction Ag/AgCl/ 3 M KCl reference electrode (type 6.0733.100, Methrom AG).

Electrode preparation. The solid-contact electrode was built on top of a glassy carbon (GC) rod (length 50 mm and diameter 3 mm) jacketed with a teflon layer. The surface of the GC disk electrode was polished first with a sheet of abrasive paper (Buehler Carbimet 600/P1200) and then with different grain-sized alumina (30, 5, 1 and 0.5 μm). Graphite oxide was prepared using a modified Hummer´s method from graphite powder (Sigma-Aldrich) by oxidation with $NaNO_3$, H_2SO_4 and $KMnO_4$ in an ice bath as reported in detail elsewhere.[17,37] A suspension of graphene oxide sheets (GO) was obtained by sonication of the prepared graphite oxide powder in distilled water (1 mg/mL) for 2 hours, followed by mild centrifugation of the suspension at 4500 rpm for 60 min.[14,38] The resulting brown-coloured water dispersion with a concentration of 0.3 mg/mL contained single to few-layered GO sheets of 2 to 10 individual layers (see Supporting Information).[38] GO films on glassy carbon (GC) electrodes were prepared as follows. Homogeneous aqueous GO dispersions of a controlled volume of 15 μL were drop-casted onto clean and polished surfaces of the GC electrodes and allowed to dry at room temperature. Once dried, the process is successively repeated to obtain GO films of controlled thickness between 125 nm and 1500 nm homogeneously covering the glassy carbon electrodes (see Supporting Information). Additionally, working with highly diluted GO dispersion of 0.01 mg/mL a 5 nm-thick deposit was drop-casted on a GC electrode (see Supporting Information). Reduction of deposited GO films was performed by a 24h exposure of electrodes to hydrazine monohydrate vapours.[18] This reduction method efficiently removes various oxygen functional groups of the graphene oxide sheets and restores the aromaticity of the carbon network, even for films as thick as 1500 nm[38]. This procedure thus transforms the GO films into reduced graphene oxide (RGO) films with remaining oxygen and nitrogen moieties of about 10 at% and 1.5 at%, respectively (see Supporting Information). For comparison purposes the XPS results of

the carboxy-functionalized graphene obtained by Jaworska et al.[35] present oxygen and nitrogen moieties of 22.6 at% and 1.2 at%.

Preparation of the ion selective membrane for calcium. An acrylic matrix was used as the base for the ion-selective membrane, the sensing part of the ISE. The acrylic matrix (methyl butyl acrylate, MBA 1:10, one portion of methyl acrylate for ten portions of butyl acrylate) was synthesized according to the procedure described by Heng et al.[39] A suitable amount of ETH129 (ionophore) and of the lipophilic salt (KTFPB) were added to the acrylic matrix following the procedure reported by Qin et al.[40] A total amount of 200 mg of cocktail (lipophilic salt, acrylic matrix and ionophore) dissolved in 2 mL of dichloromethane was used (96.5 % wt. acrylic matrix, 3 % wt. ionophore, 0.05 % wt. KTFPB). 100 μL of the cocktail-membrane was deposited by drop casting onto the glassy carbon electrode. The electrode was maintained under dry conditions for 1 day and was subsequently conditioned in the most appropriate solution depending on the measurement.

Electrode conditioning. Conditioning the electrodes is a fundamental step for obtaining reliable results. In almost all the potentiometric measurements, freshly prepared electrodes were first conditioned in a 10^{-3} M solution of $CaCl_2$ for one day in order to exchange all the interfering ions of the membrane for the target ion (Ca^{2+}) and then conditioned for two more days in a 10^{-9} M solution of $CaCl_2$ to completely clean the membrane of any interfering ions.[41] To estimate the limit of detection, the electrodes were conditioned for one day in the same solution in which the measurements were taken (different initial solutions were tested according to the dilution method proposed by Lai et al.[30]). For the selectivity studies we used the separate solution method,[42] and the concentration of Ca^{2+} and of the interfering ions was 10^{-2} M in all cases.

RESULTS AND DISCUSSION

Three RGO films of different thicknesses (1500nm, 125 nm and 5 nm) drop-casted on GC electrodes were probed by electrochemical techniques to elucidate the transduction mechanism for this type of ISE. First, cyclic voltammograms (CV) in a 0.1 M KCl solution were recorded (Figure 1a) at different scan rates in order to establish the most adequate values for this parameter in the following experiments. All the scans were repeated 5 times per measurement. The voltage window of the measurements ranged from 0.5 V to -0.5 V using in all cases a step potential of 0.005 V. Using a scan-rate of 100 mV/s cyclic voltammograms for the three different films were taken (Figure 1b). The electric current for the GC/RGO electrodes decreases with decreasing thickness of the RGO transducing layer and the cyclic voltammogram of the GC/RGO electrode which has a nominal thickness of only 5 nm practically overlaps with the one of the bare GC electrode. The behavior for the 5 nm deposit is explained by the fact that only some isolated GO flakes were drop-casted (instead of a 5 nm film covering the whole surface of the GC) while most of the GC electrode remained uncovered (Supporting Information). Underlining the importance of a full coverage of the GC electrode, the 5 nm thick deposit sample was not used anymore in the following experiments. Furthermore, the overall cyclic voltammograms are characterized by broad oxidation and reduction waves in addition to a small reduction peak at -0.3 V. Similar behavior was observed for single-walled carbon nanotubes.[43,44] No significant differences were obtained when comparing the voltammograms in presence and absence of oxygen in capacitive currents concluding that oxygen does not influence the electrochemical performance.

Electrochemical impedance spectroscopy (EIS) measurements (Figure 2) were performed in a working frequency range of 0.1 Hz to 10 KHz. Three different E_{dc}

potentials were applied in order to probe the behavior of the electrodes in currents in the redox zone and in the capacitive zone. The E_{dc} voltages selected were 0.0V, +0.2V (in the range of capacitive currents) and -0.2V (close to the reduction peak of oxygen). The amplitude of the measurements in all the cases was 10 mV, and all the solutions were bubbled with nitrogen in the same way as done for the cyclic voltammetry measurements. All impedance measurements were carried out at least three times for each GC/RGO electrode to ensure the reproducibility of all the data.

Figure 2a shows the EIS response of the 1500 nm thick RGO film tested at three different dc-potentials (E_{dc}). At low frequencies we can observe a change in the behavior of the electrodes when the potential is moved to negative values close to the reduction peak of oxygen. The presence of a semicircle in the high frequencies indicates a surface charge-transfer process followed by a capacitance phenomenon in the region of low frequencies with a phase angle less than 90°. According to the previous cyclic voltammetry measurements, EIS analyses were recorded at positive potentials (E_{dc} = +0.2 V) to avoid any possible interference due to the redox reactions of oxygen.[43] As for the cyclic voltammetry, the presence of oxygen does not influence the EIS response (Figure 2b). Figure 2c shows the impedance spectra for the GC/RGO electrodes of 125 nm and 1500 nm thickness. The dependence of the low-frequency line on RGO film thickness indicates that it originates from a bulk process within the RGO film. The magnification of the high-frequency region (inset Figure 2c) reveals a depressed semicircle.

In order to elucidate the mechanism of transduction, several equivalent electrical circuits were fitted to the experimental data by non-linear least squares fitting. The best equivalent circuit and the proposed transduction mechanism obtained are presented in Figure 3. Our equivalent circuit is different from the one proposed by Li et al.,[34] but we

have to take into account that apparently Li et al. did not perform the reduction process to form RGO from GO. In their case the proposed equivalent circuit is similar to the one using carbon nanotubes as solid transducers.[43]

The average error (χ^2) of the fits for 121 different impedance spectra for different thicknesses of the graphene layer and different supporting electrolytes was around $1x10^{-4}$. The equivalent circuit is composed of the solution resistance (R_s), an interfacial constant phase element (CPE_I) in parallel with a charge-transfer resistance (R_{ct}), and the classical Warburg diffusion element (Z_D) in series with a bulk constant phase element (CPE_B). This equivalent circuit gives excellent agreement between experimental and calculated impedances, as illustrated by the Bode plot (Figure 4).

The influence of different electrolyte concentrations on the EIS spectra is shown in Figure 5 for the 1500 nm thick film. The values of solution resistance, R_s are independent of the RGO film thickness (and of E_{dc}), and R_s is inversely proportional to the supporting electrolyte concentration, as expected (Table 1).

Opposite to R_s, the charge-transfer resistance R_{ct} is dependent on the RGO film thickness. The values for R_{ct} are significantly higher for the 125 nm films, compared with the 1500 nm thick films. This charge-transfer resistance is not related with any redox reaction because the measurements are recorded using supporting electrolytes without added redox couples at dc-potentials where possible oxygen redox processes are not present. Therefore, R_{ct} could originate from electron transfer at the GC/RGO contact or from ion transfer at the RGO/electrolyte solution interface. Since R_{ct} depends on the supporting electrolyte concentration it presumably originates from ion transfer at the RGO/solution interface

Two different capacitances (CPEs) are observed in the impedance spectra. One (CPE_I) is related to the RGO/solution interface and the other one (CPE_B) is related to

the bulk of the RGO film. The CPE parameters (Y_0 and n, frequency-independent parameters)[45] for the interfacial and bulk capacitances are collected in Table 2. Five different electrolytes (KCl, NaCl, LiCl, $NaClO_4$ and $LiClO_4$) were used to show the different behavior of the electrodes in different electrolytes and determine the values of CPEs and Warburg element.

The values of Y_0 increase for both CPEs when the thickness of RGO film increases. These Y_0 values depend dramatically on the supporting electrolytes used in the impedance measurements. The n values give information about the deviation of CPE from a real capacitor. The possible values of n are between 0 and 1, where a value of 0 means that the CPE is acting as an ideal resistor, and values of 1 as an ideal capacitor. The values observed are in the range 0.5–1 for the interfacial process (CPE_I) and they are higher to 0.9 for the bulk process (CPE_B). The depressed semicircle in the inset of Figure 2c corresponds to the constant phase element (CPE_I) in parallel with the charge-transfer resistance (R_{ct}). This system is also called Zarc element and may be caused by e.g. surface roughness, variation in the thickness or non-uniform current distribution.[45] Its phase angle is confirmed in the Bode plot presented in Figure 4. Such a constant-phase element behavior has been observed for some other carbon-based electrodes due to the roughness of the electrodes interface.[46] This agrees with the microscopic characterization made by SEM and AFM (see Supporting Information).

The occurrence of CPE behaviour (instead of ideal capacitors) can be related to the RGO material itself. RGO sheets are composed of basal and edge planes with different conductive and capacitive properties. These differences in the planes can cause time constant distributions and thus CPE behavior associated with bulk (CPE_B) and interfacial (CPE_I) charging processes. Another reason for the appearance of CPEs instead of true capacitors could be the porosity and roughness of the RGO film. The

dependence of Warburg element on the film thickness (Table 2) indicates that Z_D is related to diffusion processes in the bulk of the RGO transducing layer. When SWCNTs are used as transducer layer in electrochemical measurements,[43] basically the sensing mechanism is produced by capacitance[47] or conductance depending on the kind of sensor where SWCNTs are used. Similar behavior can be also explained in the case of RGO in a similar way. Reduction processes transform insulating GO into conductive RGO by removing oxygen containing functional groups at the basal plane and the edges, and restoring the aromaticity of the carbon network thus recovering conductivity in RGO. Since the degree of removal of oxygen functionalities and the restoration of the conductivity can be controlled by the applied reduction process,[48] in RGO both kind of mechanisms, capacitive and conductive are possible. For instance, Robinson et. al.[18] made a gas sensor device based on RGO where conductance was the transduction mechanism. In our case, RGO is acting as a capacitance-based transducer due to the double layer capacitance produced by both constant phase elements (CPE_I and CPE_B). There is no redox processes as in the case of conducting polymers[49] but RGO acts as an asymmetric capacitor where one side is formed by the ions in the solution (or in the ion selective membrane in the case of ISEs) and the other side is formed by the graphene sp^2-electrons. With this transduction mechanism, it is preferable to have a solid contact with a high capacitive value as long as the adhesion and the coverage of the glassy carbon rod remain good. Since the capacitance of RGO increases with film thickness (Table 2), the thicker RGO film (1500 nm) is preferable (compared to the 125 nm film) as ion-to-electron transducer in solid-contact ISEs.

Once we have completely characterized RGO films as transducing element in potentiometric measurements, we have placed on the top of the GC/RGO electrode an ion-selective membrane (ISM) for the detection of calcium ions (see the ‘Preparation of

the ion selective membrane for calcium' in the Experimental Part). Therefore, as a proof of concept, the ISE for the selective detection of calcium is formed by the GC/RGO/ISM electrode. Sensitivity and linear range of the electrode were calculated on the basis of 30 calibration curves with 6 different electrodes (5 measurements for each electrode) measured over more than one month, what shows the performance of these ISEs over time (Figure 6). The variation of EMF versus time is shown in Figure 6a. Time responses of approximately 5 minutes are observed for very low concentrations of Ca^{2+}. This response time decreases to a few seconds for higher concentrations of Ca^{2+}. Figure 6b shows the typical potentiometric calibration curve with an excellent Nernstian slope with values of 29.5 mV/decade (n=30, SD=0.8 mV/decade, R=0.9999) and with a linear range from 10^{-5} to $10^{-2.5}$ M. The vertical bars in Figure 6b for each level of Ca^{2+} activity represent the standard deviation obtained with 30 experimental values (6 different electrodes and 5 measurements for each electrode). The maximum of these standard deviations in the linear range is 2.32 mV, almost half of the one obtained by Jaworska et al.[35] in their carboxy-functionalized graphene-based ISE. Medium-term stability of the electrodes was evaluated by recording the potentiometric signal during 24 hours using a concentration of $10^{-2.4}$ M of $CaCl_2$ (Figure 7). The initial conditioning solution was 10^{-6} M before adding a medium concentration ($10^{-4.8}$ M) to achieve the final concentration of $10^{-2.4}$ M. We observed a very minor and stable drift of the potentiometric signal (10 μV/h) compared with ISEs based on other nanostructured materials,[31,32,50] a drift that is slightly better than the one presented by Ping et al.[33] in their RGO-based ISE. A much higher drift has been observed in a previous work using the same membrane and SWCNTs as transducer (493 μV/h)[51]. RGO seems to add more stability to the signal avoiding drifts at short and medium time responses. The increase in signal/noise ratio is a clear advantage to obtain reliable analyte concentrations. A

limit of detection of $10^{-6.2}$ M was estimated with the newly developed ISE. The limit of detection obtained in this paper is similar for other solid-contact calcium ISEs and the same obtained in a previous work using SWCNTs since limit of detection and the selectivity values are slightly influenced by the transducer layer and depend strongly on the composition of the ion-selective membrane.[52] The selectivity of the RGO-based electrodes has been compared with similar solid-contact electrodes based on different conducting polymers.[53] The results are shown in Figure 8 and the comparison of the values is collected in Table 3, where selectivity coefficients have been obtained using the separated solution method.[42]

In order to determine the presence of an aqueous layer between the RGO transducing layer and the ion-selective membrane that could influence the instrumental signal, we performed the water layer test proposed by Fibbioli et al.[27] The formation of this thin aqueous layer could cause chemical hysteresis and also mechanical failures due to the presence of ions or CO_2 in the water layer. The water layer test consists of observing the behaviour of the ISE when a solution of the primary ion ($CaCl_2$ 0.1 M in our case) is exchanged for a solution of an interfering ion ($MgCl_2$ 0.1 M in our case), and then exchanged again for the initial solution of $CaCl_2$. Potential drifts observed in any part of the changing solution procedure indicate the presence of a thin aqueous layer, which causes new equilibriums due to diffusion of ions to the aqueous layer. Electrodes were conditioned in a $CaCl_2$ 0.1 M solution for 24 hours and then replaced with a fresh solution of $MgCl_2$. Figure 9 shows a very stable response testing all the three different zones. Very fast shifts are observed when the primary ion (zone A) is replaced with an interfering ion (zone B), and also when this ion is replaced for the initial solution (zone A). This fact suggests that the calcium is rapidly replaced by magnesium in the membrane. The water layer is presumed to be absent because there are no appreciable

drifts in zone B due to the equilibrium of the interfering ion in the aqueous layer.

In a previous work using a nanostructured material (3DOM)[30] as transducer, Lai et al. observed a positive drift when a solution of the primary ion was exchanged for an interfering ion, probably due to the leaching of the primary ion from the PVC membranes, but this effect has not been shown in our ISE, obtaining a very fast replacement of primary ions without any drift. Similar results were obtained using SWCNTs with the same membrane in a previous work.[51] Both graphene and SWCNTs based ISEs displays a highly hydrophobic behavior that probably prevents the formation of aqueous layer in the electrodes.[54]

Conclusions

In this work we presented the use of reduced graphene oxide (RGO) films as transducer material in potentiometric all-solid-state ion-selective electrodes (ISE). Good adhesion to the underlying glassy carbon electrode, homogeneous coverage and high capacitive values were obtained for RGO films with thicknesses of 125 nm and 1500 nm. The transduction mechanism revealed that RGO films act as asymmetric capacitors with high capacitive values. As a proof of concept, the GC/RGO-film electrodes were used in the construction of an ISE for calcium. Highly reproducible sensing responses over time with outstanding increased signal-to-noise ratio with drifts of only 10 μV/h were obtained. This provides RGO films with advantages over other types of transducer materials such as conducting polymers and carbon nanotubes. Combined with the ease of fabrication of RGO films with controlled thickness on GC electrodes reliable ISE sensors with improved performance can be envisaged.

ACKNOWLEDGEMENT. This study has been supported by the Spanish Ministry of Science and Innovation (MICINN) through project grants CTQ2010-18717, MAT2010-15026, CSIC under project 201080E124 and the Government of Aragon and the

European Social Fund under project DGA-FSE-T66 CNN. CV thanks MICINN and the European Social Fund for a post-doc contract under Juan de la Cierva Programme. P.J is grateful for his PhD grant from Fundación Ramón Areces.

SUPPORTING INFORMATION. Supporting Information Available: Characterization of graphene oxide and graphene oxide films on glassy carbon electrodes. This material is available free of charge via the Internet at **http://pubs.ac.org**.

REFERENCES

(1) Yu, A.; Ramesh, P.; Itkis, M. E.; Bekyarova, E.; Haddon, R. C. *Journal of Physical Chemistry C* **2007**, *111*, 7565.

(2) Nair, R. R.; Blake, P.; Grigorenko, A. N.; Novoselov, K. S.; Booth, T. J.; Stauber, T.; Peres, N. M. R.; Geim, A. K. *Science* **2008**, *320*, 1308.

(3) Bunch, J. S.; van der Zande, A. M.; Verbridge, S. S.; Frank, I. W.; Tanenbaum, D. M.; Parpia, J. M.; Craighead, H. G.; McEuen, P. L. *Science* **2007**, *315*, 490.

(4) Novoselov, K. S. *Science* **2004**, *306*, 666.

(5) Stoller, M. D.; Park, S. J.; Zhu, Y. W.; An, J. H.; Ruoff, R. S. *Nano Letters* **2008**, *8*, 3498.

(6) Pumera, M. *Chemical Society Reviews* **2010**, *39*, 4146.

(7) Alwarappan, S.; Liu, C.; Kumar, A; Li, C.-Z. *Journal of Physical Chemistry C* **2010**, 114, 12920.

(8) Alwarappan, S.; Boyapalle, S; Kumar, A; Li, C.-Z.; Mohapatra, S. *Journal of Physical Chemistry C* **2012**, 116, 6556.

(9) Alwarappan, S.; Joshi, R.K.; Ram, M.K.; Kumar, A. *Applied Physical Letters* **2012**, 96, 263702.

(10) Wang, Y.; Li, Y.; Tang, L.; Lu, J.; Li, J. *Electrochemistry Communications* **2009**, *11*, 889.

(11) Blake, P.; Brimicombe, P. D.; Nair, R. R.; Booth, T. J.; Jiang, D.; Schedin, F.; Ponomarenko, L. A.; Morozov, S. V.; Gleeson, H. F.; Hill, E. W.; Geim, A. K.; Novoselov, K. S. *Nano Letters* **2008**, *8*, 1704.

(12) Liu, C.; Alwarappan, S.; Chen, Z.; Kong, X.; Li, C.-Z.. *Biosensors and Bioelectronics* **2010**, 25, 1829.

(13) Ruoff, R. *Nature Nanotech.* **2008**, *3*, 10.

(14) Li, D.; Müller, M. B.; Gilje, S.; Kaner, R. B.; Wallace, G. G. *Nat. Nanotechnol.* **2008**, *3*, 101.

(15) Stankovich, S.; Dikin, D. A.; Piner, R. D.; Kohlhaas, K. A.; Kleinhammes, A.; Jia, Y.; Wu, Y.; Nguyen, S. T.; Ruoff, R. S. *Carbon* **2007**, *45*, 1558.

(16) Dreyer, D. R.; Park, S.; Bielawski, C. W.; Ruoff, R. S. *Chemical Society Reviews* **2010**, *39*, 228.

(17) Hummers, W. S.; Offeman, R. E. *Journal of the American Chemical Society* **1958**, *80*, 1339.

(18) Robinson, J. T.; Perkins, F. K.; Snow, E. S.; Wei, Z.; Sheehan, P. E. *Nano Letters* **2008**, *8*, 3137.

(19) Shao, Y. Y.; Wang, J.; Wu, H.; Liu, J.; Aksay, I. A.; Lin, Y. H. *Electroanalysis* **2010**, *22*, 1027.

(20) Pumera, M. *Materials Today* **2011**, *14*, 308.

(21) Banks, C. E.; Crossley, A.; Salter, C.; Wilkins, S. J.; Compton, R. G. *Angewandte Chemie-International Edition* **2006**, *45*, 2533.

(22) Fowler, J. D.; Allen, M. J.; Tung, V. C.; Yang, Y.; Kaner, R. B.; Weiller, B. H. *Acs Nano* **2009**, *3*, 301.

(23) Lu, G.; Ocola, L. E.; Chen, J. *Applied Physics Letters* **2009**, *94*.

(24) Li, J.; Guo, S.; Zhai, Y.; Wang, E. *Electrochemistry Communications* **2009**, *11*, 1085.

(25) Alwarappan, S.; Erdem, A.; Liu, C.; Li, C.-Z. *Journal of Physical Chemistry C* **2009**, *113*, 8853.

(26) Bobacka, J. *Analytical Chemistry* **1999**, *71*, 4932.

(27) Fibbioli, M.; Morf, W. E.; Badertscher, M.; de Rooij, N. F.; Pretsch, E. *Electroanalysis* **2000**, *12*, 1286.

(28) Lindfors, T. *Journal of Solid State Electrochemistry* **2009**, *13*, 77.

(29) Vazquez, M.; Bobacka, J.; Ivaska, A.; Lewenstam, A. *Sensors and Actuators B-Chemical* **2002**, *82*, 7.

(30) Lai, C.-Z.; Joyer, M. M.; Fierke, M. A.; Petkovich, N. D.; Stein, A.; Buhlmann, P. *Journal of Solid State Electrochemistry* **2009**, *13*, 123.

(31) Crespo, G. A.; Macho, S.; Xavier Rius, F. *Analytical Chemistry* **2008**, *80*, 1316.

(32) Parra, E. J.; Crespo, G. A.; Riu, J.; Ruiz, A.; Rius, F. X. *Analyst* **2009**, *134*, 1905.

(33) Ping, J.; Wang, Y.; Wu, J.; Ying, Y. *Electrochemistry Communications* **2011**, *13*, 1529.

(34) Li, F.; Ye, J.; Zhou, M.; Gan, S.; Zhang, Q.; Han, D.; Li, N. *Analyst* **2012**, 137, 618.

(35) Jaworska, E.; Lewandowski, W.; Mieczkowski, J.; Maksymiuk, K.; Michalska, A. *Talanta*, **2012**, 97, 414.

(36) Jaworska, E.; Lewandowski, W.; Mieczkowski, J.; Maksymiuk, K.; Michalska, A. *Analyst*, **2012**, 137, 1895.

(37) Vallés, C.; Jiménez, P.; Muñoz, E.; Benito, A. M.; Maser, W. K. *The Journal of Physical Chemistry C* **2011**, *115*, 10468.

(38) Vallés, C.; Núñez, J. D.; Benito, A. M.; Maser, W. K. *Carbon* **2011**, *50*, 835.

(39) Heng, L. Y.; Hall, E. A. H. *Analytica Chimica Acta* **2000**, *403*, 77.

(40) Qin, Y.; Peper, S.; Radu, A.; Ceresa, A.; Bakker, E. *Analytical Chemistry* **2003**, *75*, 3038.

(41) Lindner, E.; Umezawa, Y. *Pure Appl. Chem.* **2008**, *80*, 85.

(42) Bakker, E.; Pretsch, E.; Bühlmann, P. *Analytical Chemistry* **2000**, *72*, 1127.

(43) Crespo, G. A.; Macho, S.; Bobacka, J.; Rius, F. X. *Analytical Chemistry* **2009**, *81*, 676.

(44) Tang, L.; Wang, Y.; Li, Y.; Feng, H.; Lu, J.; Li, J. *Advanced Functional Materials* **2009**, *19*, 2782.

(45) Barsoukov, E.; Macdonald, J. R. *Impedance Spectroscopy Theory, Experiment, and Applications*, 2nd ed.; J. Wiley & Sons, Inc., Hoboken: New Jersey, 2005.

(46) Kim, C. H.; Pyun, S.; Kim, J. H. *Electrochimica Acta* **2003**, *48*, 3455.

(47) Snow, E. S.; Perkins, F. K.; Houser, E. J.; Badescu, S. C.; Reinecke, T. L. *Science* **2005**, *307*, 1942.

(48) Gilje, S.; Han, S.; Wang, M.; Wang, K. L.; Kaner, R. B. *Nano Letters* **2007**, *7*, 3394.

(49) Bobacka, J. *Electroanalysis* **2006**, *18*, 7.

(50) Ampurdanes, J.; Crespo, G. A.; Maroto, A.; Angeles Sarmentero, M.; Ballester, P.; Xavier Rius, F. *Biosens. Bioelectron.* **2009**, *25*, 344.

(51) Hernández, R.; Riu, J.; Rius, F. X. *Analyst* **2010**, *135*, 1979.

(52) Mousavi, Z.; Bobacka, J.; Lewenstam, A.; Ivaska, A.; *Journal of Electroanalytical Chemistry*, **2009**, 633, 246.

(53) Michalska, A.; Konopka, A.; Maj-Zurawska, M. *Analytical Chemistry* **2003**, *75*, 141.

(54) Sun, Y.-P.; Fu, K.; Lin, Y.; Huang, W. *Accounts of Chemical Research* **2002**, *35*, 1096.

TABLE CAPTIONS

Table 1. Solution resistance (R_s) and charge-transfer resistance (R_{ct}) obtained for two different RGO film thickness electrodes in three different electrolyte concentrations.

Table 2. Interfacial constant phase element (CPE_I), bulk constant phase element (CPE_B) and Warburg (Z_D) element values obtained for two electrodes with different RGO film thicknesses in different electrolytes.

Table 3. Comparison of experimental selectivity coefficients log $K_{Ca,J}^{Pot}$ for different ISEs.

Table 1

Solutions	Film thickness (nm)	R_s (Ω)	R_{ct} (Ω)
KCl 0.01 M	1500	62.4 ± 0.4	35.5 ± 1.7
	125	64.2 ± 0.3	92.5 ± 0.3
KCl 0.05 M	1500	15.1 ± 0.2	6.8 ± 0.4
	125	10.3 ± 1.5	135 ± 0.7
KCl 0.1 M	1500	6.9 ± 0.0	8.7 ± 0.4
	125	4.8 ± 0.1	75.6 ± 3.1

Table 2

Solutions (0.1M)	Film thick-ness (nm)	CPE_I		CPE_B		Z_D [c]
		CPE_I, Y_0 [a]	CPE_I, n [b]	CPE_B, Y_0	CPE_B, n	
KCl	1500	0.00017	0.9839	0.00437	0.9436	0.004
	125	0.00009	0.6552	0.00014	0.9173	0.001
NaCl	1500	0.00282	0.5939	0.02150	0.9237	0.02
	125	0.00003	0.7631	0.00056	0.9296	0.0005
LiCl	1500	0.00426	0.5491	0.10062	0.9283	0.01
	125	0.00004	0.7006	0.00014	0.9020	0.0001
$NaClO_4$	1500	0.01481	0.5530	0.19865	0.9142	0.02
	125	0.00002	0.8368	0.00042	0.9432	0.004
$LiClO_4$	1500	0.00192	0.7500	0.01480	0.9340	0.01
	125	0.00003	0.7809	0.00057	0.9314	0.0005

[a] Values of Y_0 are given in $S \cdot sec^n/cm^2$

[b] adimensional

[c] Values for Warburg element are given in $S \cdot sec^{0.5}/cm^2$

Table 3

Ion	Slope ± s[a] (mV/dec)	RGO	SWCNTs[43]	Internal Filling Solution[44]	Cond. Pol.[44]	Modified Conducting Polymer[44]	PPy (Tiron)[47]
Mg^{2+}	29.0 ± 0.1	-5.3	-4.8	-3.4	-3.7	-5.2	-6.5
Ba^{2+}	28.1 ± 0.1	-5.1	-5.5	-3.3	-3.1	-3.3	-3
Li^{+}	43.5 ± 0.2	-3.5	-2.5	-1.1	-1.7	-2	-1.9
K^{+}	35.1 ± 0.3	-3.1	-2.2	-0.9	-1	-1.1	-2.2
Na^{+}	44.9 ± 0.2	-3.0	-3.1	-1.5	-2.5	-2.6	-1.9

[a] values of standard deviation obtained for 2 replicates for 6 different electrodes

FIGURE CAPTIONS

Figure 1. Cyclic voltammograms for GC/RGO electrodes in a 0.1 M KCl solution in the voltage window from -0.5 V to 0.5 V. a) for the 1500 nm thick RGO film at different scan rates (5, 10, 20, 50, 100, 200 and 500 mV/s). b) for the 1500 nm, 125 nm, and 5 nm thick RGO films at a scan rate of 100 mV/s.

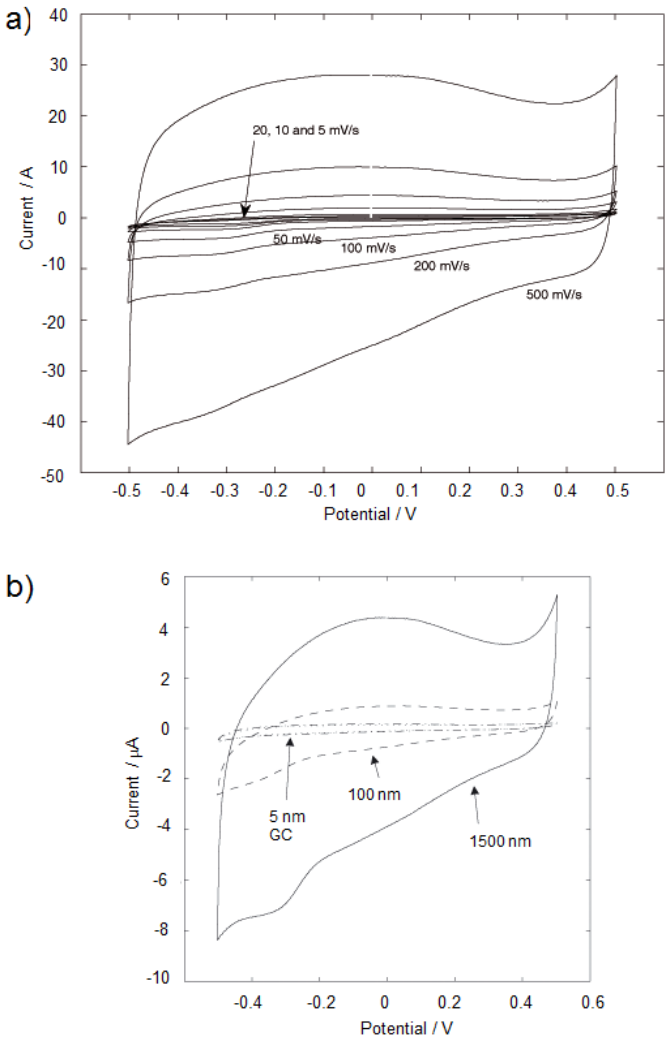

Figure 2. EIS spectra for the GC/RGO electrodes in 0.1 KCl solution. Frequency range: 0.1 Hz to 10 kHz. a) E_{dc} dependence for the 1500 nm thick RGO film: +0.2V (squares), 0.0V (triangles) and -0.2V (circles) (Inset: magnification of high frequency region showing characteristic semicircle for Zarc circuits). b) Oxygen dependence: EIS spectra for 1500 nm thick RGO film before (filled circles) and after (empty circles) nitrogen bubbling (E_{dc} = +0.2 V). c) Thickness dependence: EIS spectra for the 125 nm and 1500 nm thick RGO film for the 125 nm (circles) and 1500 nm (squares) thick RGO electrodes (E_{dc} = +0.2 V).

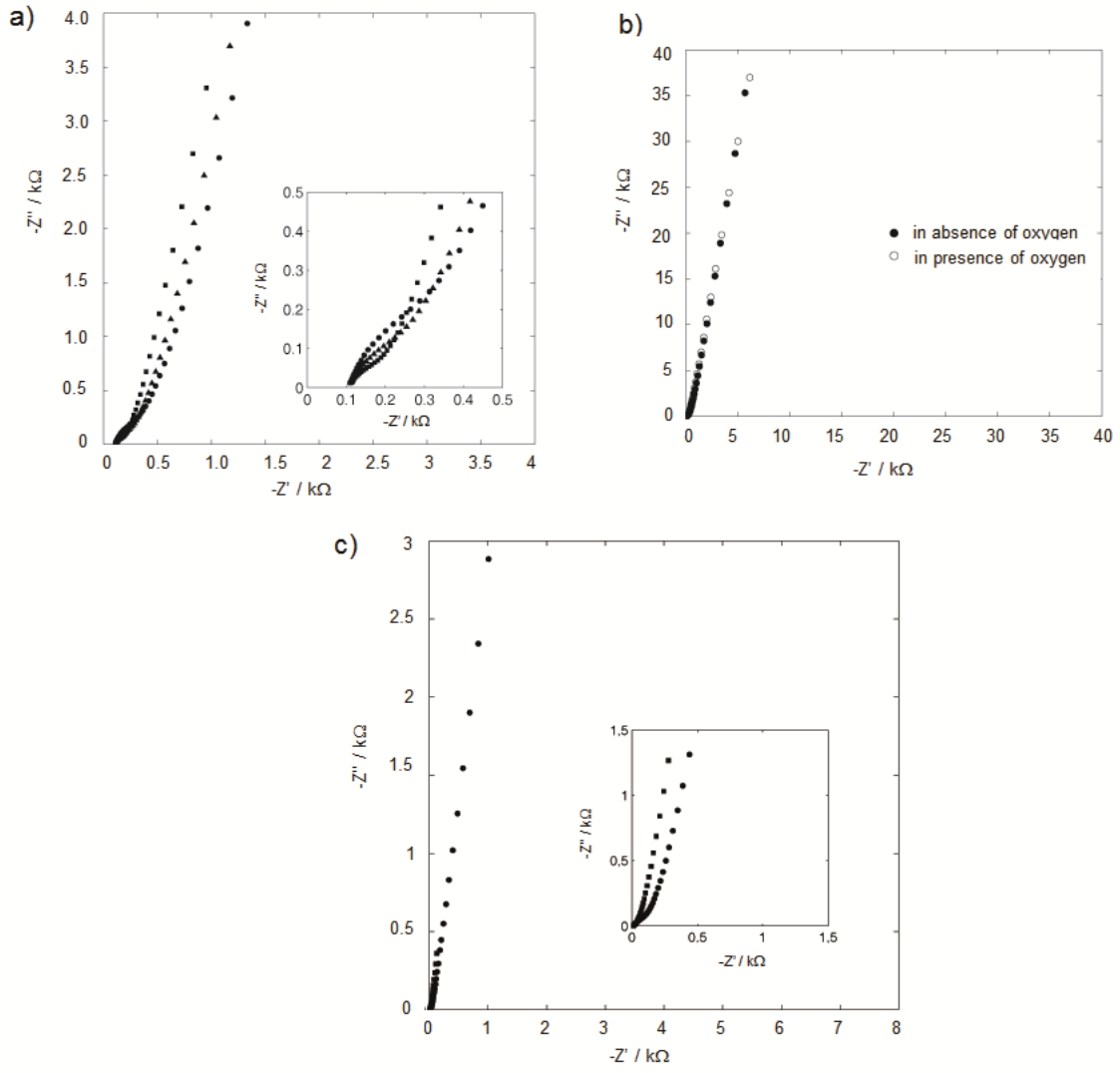

Figure 3. Proposed mechanism involved in the ion-to-electron RGO transduction and equivalent circuit for the GC/RGO electrodes. In the figure the RGO flakes are much smaller than the area of the conducting wire beneath them and the flakes are interconnected.

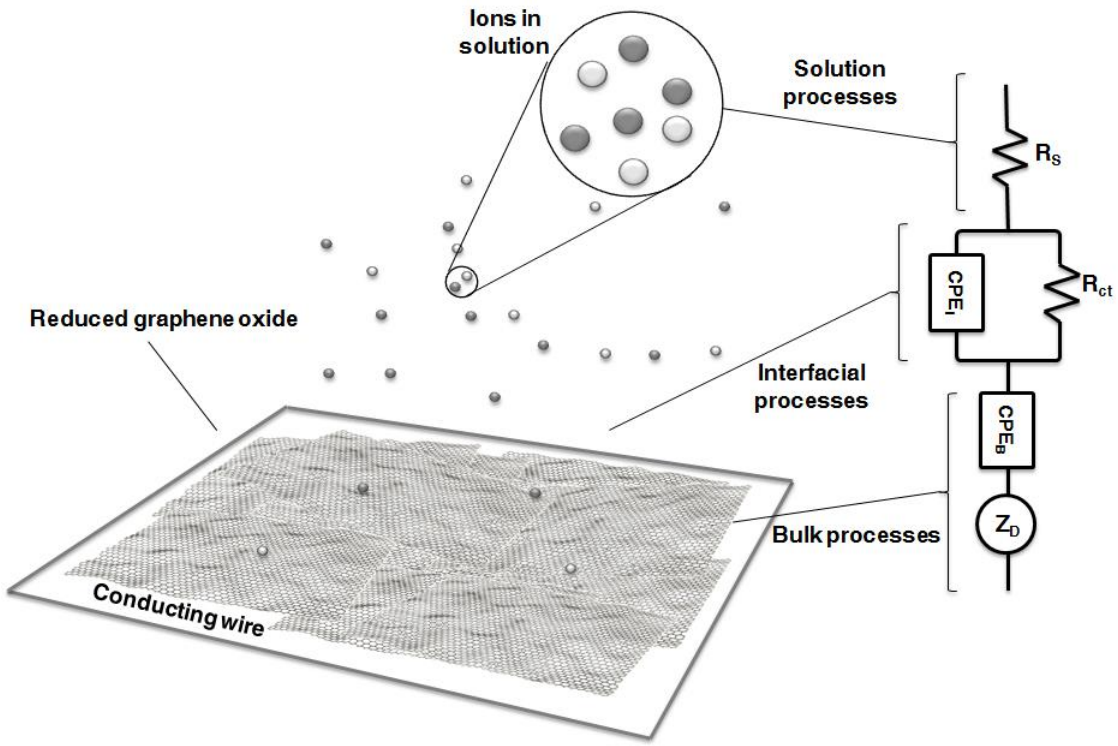

Figure 4. Bode plot of GC/RGO film electrodes in 0.1 M KCl solution. E_{dc}=+0.2 V, excitation amplitude of 10 mV, frequency range: 0.1 Hz to 10 kHz, graphene film thickness = 1500 nm. The empty symbols are the fitted values for the experimental data using the equivalent circuit from Figure 3.

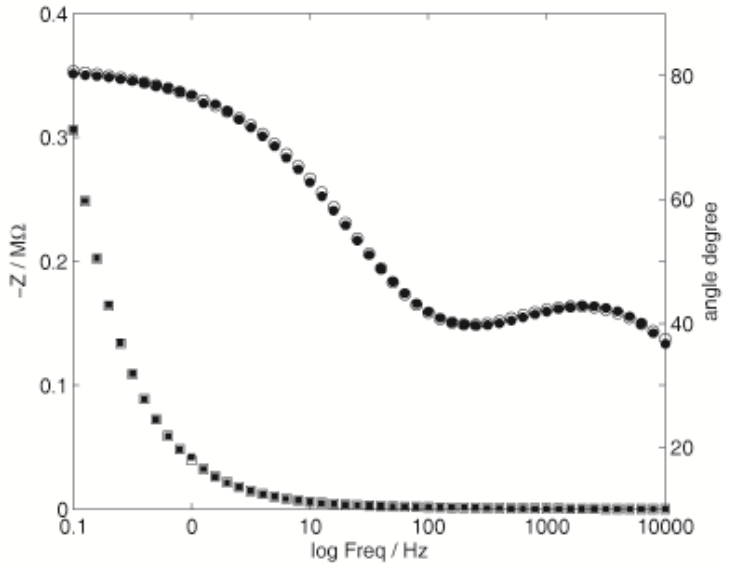

Figure 5. Electrochemical impedance spectra for GC/RGO 1500 nm film thickness electrodes in (circles) 0.1 M KCl, (squares) 0.05 M KCl and (triangles) 0.01 M KCl (E_{dc} = +0.2 V, frequency range: 0.1 Hz to 10 kHz).

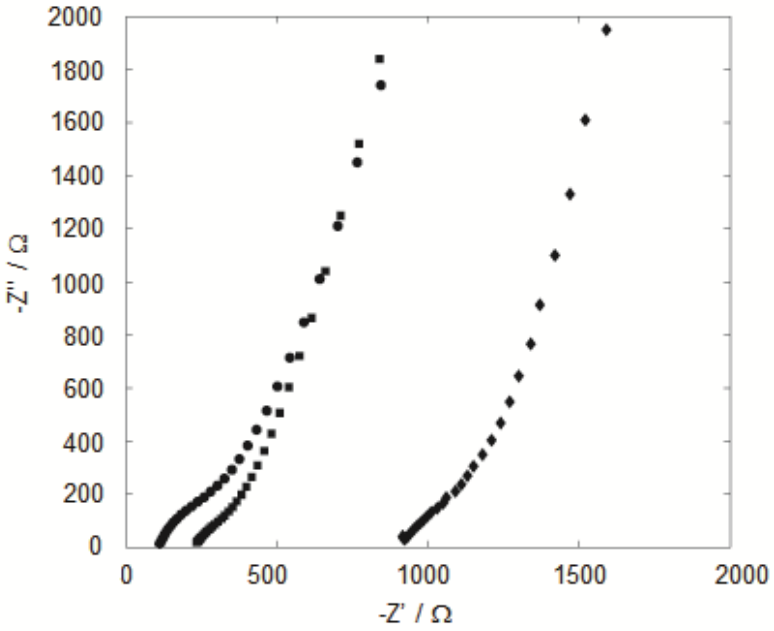

Figure 6. GC/RGO/ISM as ISE for Ca^{2+} detection. a) Potentiometric time response of RGO Ca^{2+}-selective electrode for different Ca^{2+} activities. Inset: Time response for low concentrations (10^{-6} M). b) Nernstian slope of RGO-based Ca^{2+}-selective electrodes. The bars indicate standard deviations.

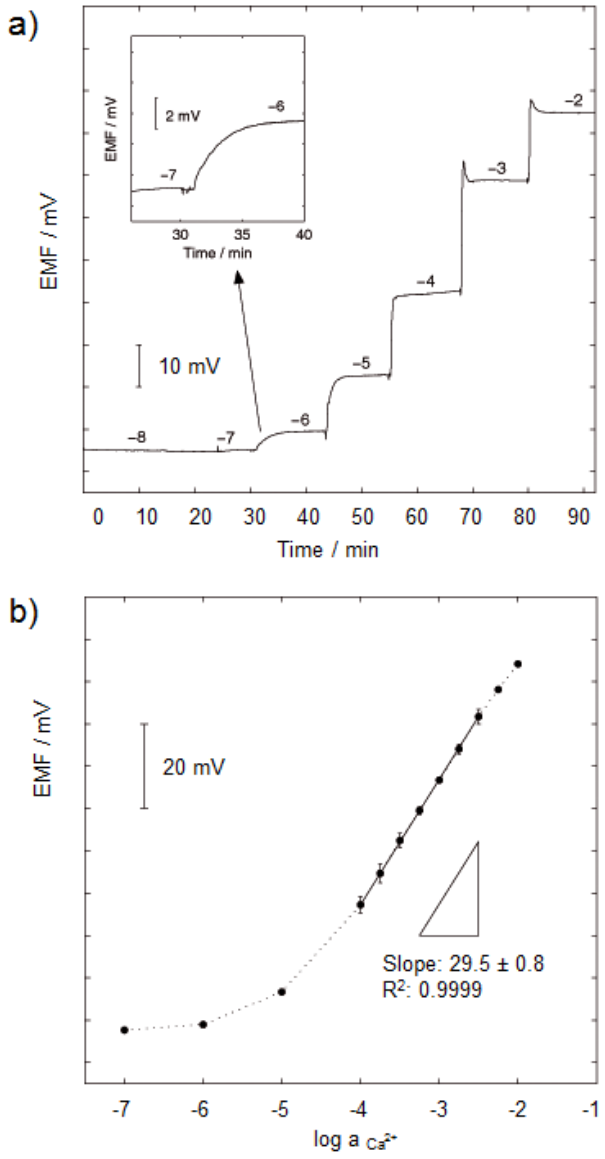

Figure 7. Medium term potential stability of the Ca^{2+}-selective electrode over 24 hours for a $10^{-2.4}$ M solution of $CaCl_2$.

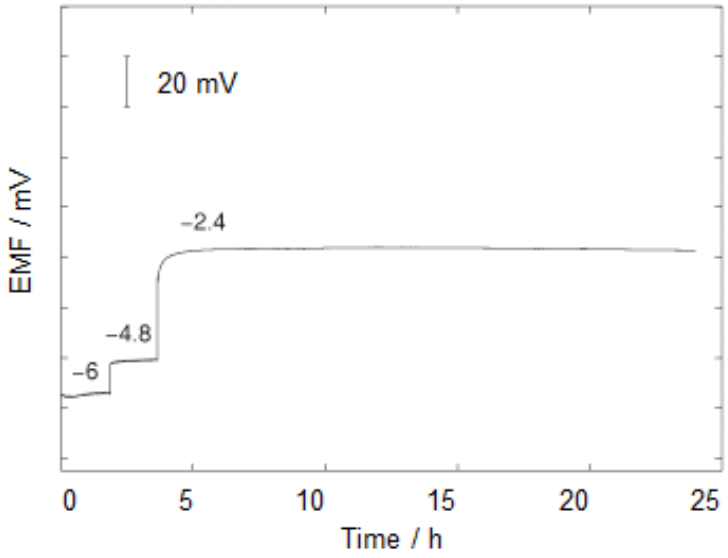

Figure 8. Comparison of the different selective coefficients for ISEs based on RGO, SWCNTs and conducting polymers.

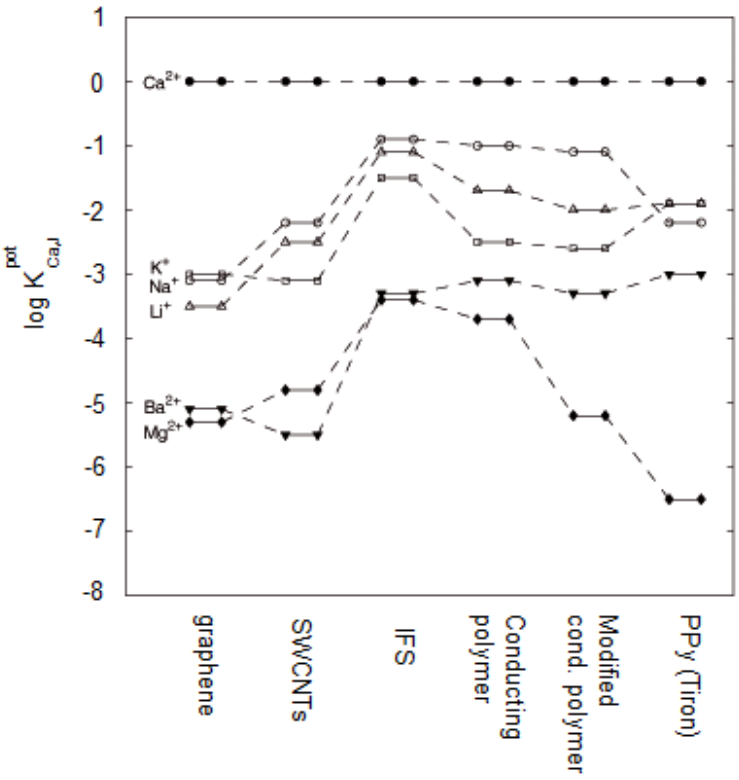

Figure 9. Potentiometric response of ISE in the water layer test: (A) at t=1 hour, the 0.1 $CaCl_2$ fresh solution of primary ion was replaced for the interfering 0.1 $MgCl_2$ solution. (B) At t=4 hours, the interfering solution was exchanged for the initial solution observing a very stable signal to 24 hours.

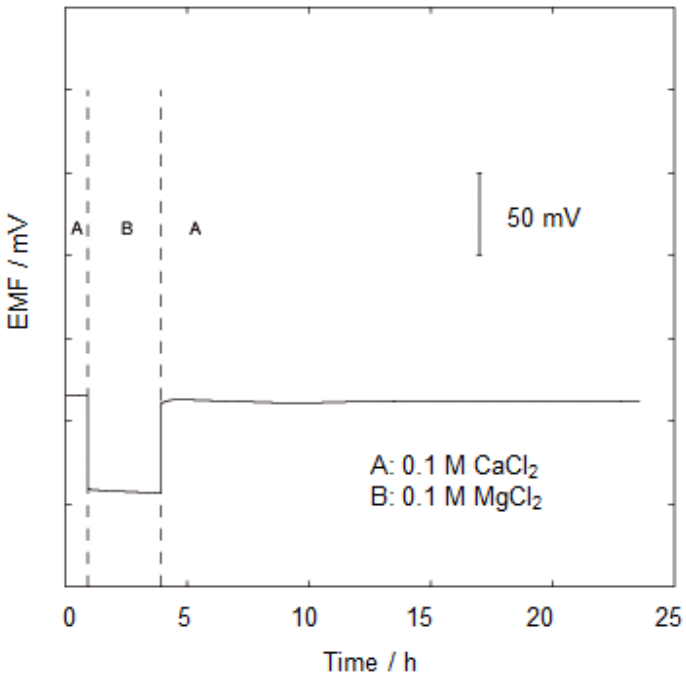

TOC Image

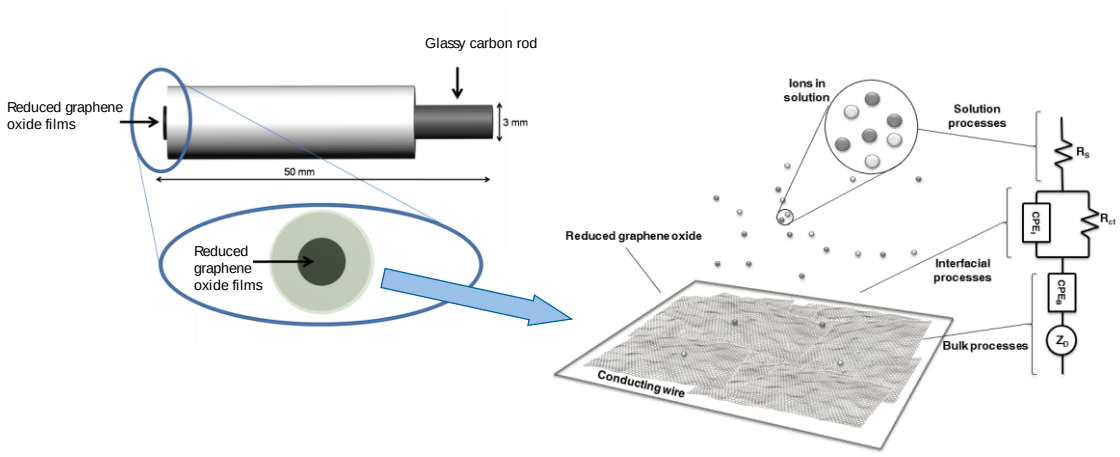
Glassy carbon rod
Reduced graphene oxide films
3 mm
50 mm
Reduced graphene oxide films
Ions in solution
Solution processes
Reduced graphene oxide
Interfacial processes
Bulk processes
Conducting wire